A 3D interpolation algorithm for layered tilted geological formations using an adapted inverse distance weighting approach

M. WALTHER, N. BÖTTCHER & R. LIEDL
Technische Universität Dresden, Institute for Groundwater Management, D-01062 Dresden, Germany
marc.walther@tu-dresden.de

Abstract We present an algorithm for the 3D interpolation of layered tilted hydro-geological structures from point data. The method uses profile information and interpretations of the geological layering to interpolate discrete or continuous values in a meshed grid consisting of arbitrary element types. The user has the opportunity to tweak several options of the algorithm depending on the given application's circumstances (e.g. data availability and reliability) and additional soft information of the geology. The interpolation algorithm is implemented in Qt and can be used as a pre-processing tool for mesh-based numerical methods (i.e. finite difference method, finite element method, finite volume method).

Key words interpolation; 3D; pre-processing; inverse distance weighting; tilted; layered

INTRODUCTION

It is a common practice to use numerical models as tools for the reproduction of a current state or the prediction of future scenarios. The more data is known from measurements, the more detailed the model that can be set up. In most real-world applications of numerical models, several limitations restrain data acquisition, as measurements take time, need funding, or may not be realizable, e.g. the location where to measure cannot be reached. Also, it is not feasible to obtain the parameterization by measurements for every single model discretization point, although it is needed to run the model. When dealing with such limited data availability, interpolation becomes necessary for the model setup and the incorporation of the real-world data.

Interpolation methods

Frequently used interpolation methods in geosciences are kriging (Bargaoui & Chebbi, 2009), inverse distance weighting (IDW, Lu & Wong, 2008), triangulation (Watson, 1982) or spline interpolation (Dubrule, 1984), each differing in complexity, data requirements and user effort. These basic interpolation methods are sometimes combined with additional techniques, e.g. fuzzy neural networks (Ayvaz *et al.*, 2007), and altered or extended to fit individual task-related requirements (Yue *et al.*, 2007). For manifold applications, a vast number of 2D implementations (mostly surface data interpolation) can be found, e.g. thematic interpolation (Bartier & Keller, 1996) or adaptive enhanced exponent interpolation (Lu & Wong, 2008). Three-dimensional interpolation applications are found less frequently and often require increased computational effort; among these, some are grid-based approaches (Falivene *et al.*, 2007), use quality information (Rühaak, 2006) or cross-sections as the data basis (Ming *et al.*, 2010), or utilize potential-field data to include additional soft-data knowledge for the interpolation (Calcagno *et al.*, 2008). In most cases, the approach focuses on a specific feature to be resembled in the interpolation, e.g. folded structures, fractures, etc. As most groundwater models deal with rather simple geological structures, i.e. layered sediment deposits, complex interpolation models are not required. In this article we present a simple approach to describe layered deposits while including known tilted structures from borehole interpretations within a 3D space.

METHODS AND IMPLEMENTATION

Interpolation Algorithm (IA)

The user needs to provide borehole information and the geological interpretation of the layered structures, from which the latter is done by "pointing" from one layer in a first profile to another

layer in a second profile (compare Fig. 1). The interpolation domain needs to be available as a pre-meshed grid. The IA uses the following procedure:

(1) From the user-specified borehole information, IA creates a list of points in x-y-dimension (profile points, PP) each containing the given layer information in vertical direction. From the given layer information, IA will distribute layer points (LP) for each PP.
(2) For each grid point (GP), which is the centre of a mesh cell, IA searches for PP within a given horizontal circular extent.
(3) Within each found PP, projected layer points (LP′) are created by applying a coordinate transformation to the LP in relation to the GP following equations (1)–(4); LP′ will differ from LP in elevation (Δz in Fig. 2) depending on the given tilting (angle α) of the associated geological layer formation (compare Figs 1–3). IA looks for LP′ within a given vertical extent from the GP elevation. In case IA will not find a given minimum number of LP′, the user may apply the option to increase horizontal and/or vertical search boundaries until a maximum number of repetitions.

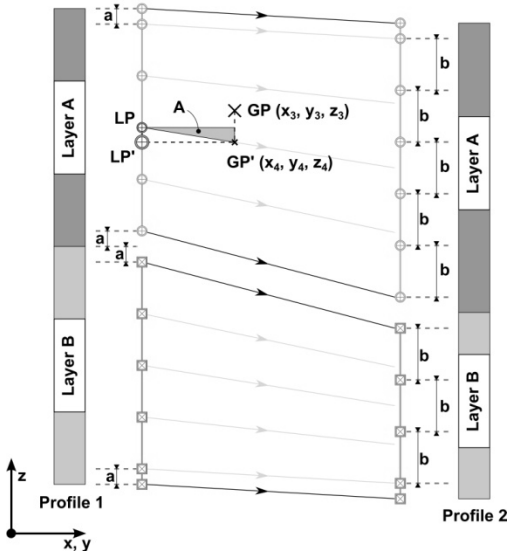

Fig. 1 Vertical cross-section of example profile 1 and 2 with different hydro-geological layer sizes; layers A and B of profile 1 are "pointing" towards the respective layers in profile 2. In profile 1, (a) depicts the layer border interval, in profile 2, (b) depicts the layer distribution interval.

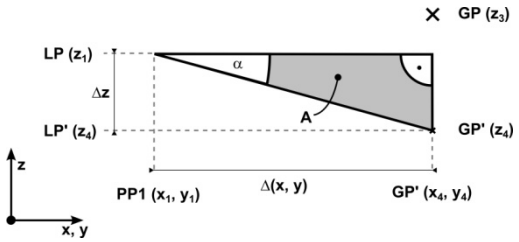

Fig. 2 Triangle A from Fig. 1 enlarged, not to scale.

Let *S* be a planar surface originating from one LP in profile 1 with the horizontal angle β as the deviation from the x-axis and the vertical angle α as the deviation from the z-axis, both obtained from the user specified "pointing" information (i.e. the tilting of a layer to another one). From Fig. 2 it can be seen, that the needed vertical displacement Δz of LP′ from LP is:

$$\Delta z = \Delta(x, y) \cdot \tan \alpha \tag{1}$$

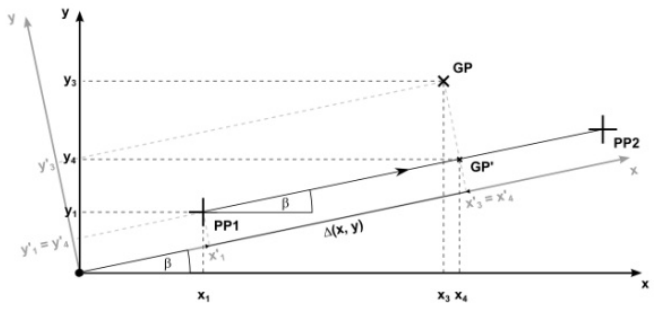

Fig. 3 Horizontal plain showing coordinate transformation of GP to GP′ for determination of elevation of LP′.

To determine the horizontal distance $\Delta(x,y)$, which is the line segment between LP′ and GP′, the coordinates (x_4, y_4) of GP′ are obtained as depicted in Fig. 3 via:

$$\begin{aligned} x_4 &= x_3^{'} \cdot \cos\beta - y_1^{'} \cdot \sin\beta \\ y_4 &= x_3^{'} \cdot \sin\beta + y_1^{'} \cdot \cos\beta \end{aligned} \tag{2}$$

with

$$\begin{aligned} x_3^{'} &= x_3 \cdot \cos\beta + y_3 \cdot \sin\beta \\ y_1^{'} &= -x_1 \cdot \sin\beta + y_1 \cdot \cos\beta \end{aligned} \tag{3}$$

and by substituting:

$$\begin{aligned} x_3^{'} &= x_4^{'} \\ y_1^{'} &= y_4^{'} \end{aligned} \tag{4}$$

The position of the projected grid point (GP′) is found by vertically relocating GP on *S* and following *S* to the line segment between the profile points PP1 and PP2 while not changing the elevation.

(4) IA produces a priority list of the found LP′ sorted according to the weighting by their inverse distance multiplied by a user-specified custom weighting factor; the last gives the hydro-geologically experienced user the option to declare some layers to be more or less certain.

(5) Depending on whether the interpolation uses discrete or continuous values, IA individually sums up the weightings of the found discrete values and chooses the discrete value with the maximum weighting sum as the grid cells' interpolation value or sums the multiplications of the continuous value by the related inverse distance weighting, respectively, as in equations (5)–(7).

$$x_{\text{interpol}} = \sum_i x_i w_i \tag{5}$$

with x_{interpol} being the interpolated value at a grid cell, x a given value at a LP′ and w the standardized weighting at the found LP′ with:

$$w = \frac{w^*}{\sum_i w_i^*} \tag{6}$$

and

$$w^* = \frac{\sum_i d_i}{d} \tag{7}$$

with d as the distance between the grid cell and the found layer point.

IA features and implementation

The user is given a limited number of parameters to adjust. As an interpolation can only be an interpretation of the natural conditions (within the given hydrogeological subject), the following parameters allow the user to influence the outcome of the interpolation to fit her/his interpretation.

(a) Minimum number of LP′ to be used for the calculation of the interpolation value.
(b) Number of repetitions to search for LP′ and to multiply the search boundaries with their respective search extension factors.
(c) Factor of horizontal and vertical search boundary extension, if the number of LP′ found is smaller than (a).
(d) Layer border and layer distribution interval (compare Fig. 1); the LP of a profile are distributed in the following way: The boundary between two known geological layers receives with a distance of the layer border interval two LP, one above and one below the boundary. Between these LP at the boundaries, additional LP are distributed equally with the layer distribution interval. The smaller these two values, the more precise the interpolation outcome will be, but the longer the computation will take.
(e) Horizontal circular and vertical search boundary around the centre coordinates of a GP.
(f) Choice, if the variable is of logarithmic type (e.g. hydraulic conductivity).
(g) The user may utilize a "critical distance weighting" (CDW). This will offer a way to describe the inverse distance weighting function by three parameters, a weighting value at a critical distance ($\varepsilon_{(d_{\mathrm{crit}})}$) and a shape factor *a* of the weighting function (see equation (8) and Fig. 4). It is also possible to let IA choose d_{crit} based on the given distribution of the borehole information as the mean of the minimum PP distances. When the given PP are distributed cluster-like throughout the interpolation domain, CDW helps to produce better interpolation results within the PP clusters, which show a smaller grid size scale. The weighting function is given by:

$$\varepsilon = a^{\zeta} \tag{8}$$

with $\zeta = -d^{b}$, while *d* is distance from LP′, ε is weighting value ($0 < \varepsilon < 1$), *a* is shape factor ($a > 1$), and *b* is internal parameter determined on runtime by inverting equation (8) and setting $d = d_{\mathrm{crit}}$.

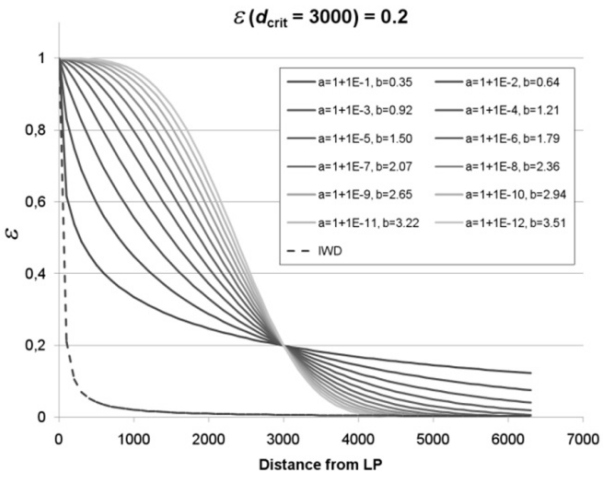

Fig. 4 Reduction of CDW weighting function for different shape factors in comparison to IDW weighting function.

The user can review the outcome and quality of the interpolation via the additional output of the IA, which includes for each GP: number of times the search boundary had to be extended when

minimum number of LP′ were not found, actual search boundaries resulting from the search boundary extension (horizontal and vertical), weighting and value of first three interpolated values of highest priority for discrete interpolation, number of LP′ used for interpolated value, and a qualitative information "imaginary interpolation insecurity" (III) expressing how uncertain the interpolated value is:

$$\mathrm{III} = V^{p} \tag{9}$$

with $V = \pi \cdot r_a^2 \cdot h_a$ as "search volume" of a GP, while r_a is actual horizontal circular search boundary, h_a is actual vertical search boundary and $p = (1 + n_{\mathrm{SBinc}})/n_{\mathrm{LP}}$ and n_{SBinc} is number of times search boundaries had to be increased as minimum number of LP′ were not found and n_{LP} is number of LP′ found. The larger III, the more "insecure" the interpolated value is supposed to be. The value of III will increase with greater search volumes and number of times of search boundary extension and will decrease with more LP′ found.

The IA code is implemented in the cross-platform application framework Qt (a C++ class library) providing a graphical user interface and a couple of help texts and images.

APPLICATION

In the following, two applications will be shown using a synthetic example and real-world data for discrete interpolation of sedimentary structures.

Synthetic example

To demonstrate the applicability of the IA, Fig. 5 shows the position of five imaginary boreholes and the hydro-geological layer information including five discrete materials. Figure 6 depicts a possible interpretation layered structure for the cross section a-b-c-d, which is used as input data for IA. Figures 7–9 present the outcome of the interpolation.

Comparing the two vertical cross sections from Fig. 6, i.e. the provided input data, and Fig. 7, i.e. the interpolation result, a close reproduction of the given information is obtained by the IA's output, visualizing clear material boundaries, layering and tilting of the hydro-geological structures. Figure 8 shows a 3D extension of the sedimentary structures revealing a possible development of the hydro-geology, e.g. the transition zone from material 2 to 1 between the profiles a and e. However, some minor deviations occur in areas afar from the given profile information, which is also resembled by the parameter III in Fig. 9, where darker areas at the edges of the domain depict results that are less reliable than lighter areas around the profiles. The usage of III can aid the user to carefully review the interpolation results in the extrapolated zones of the domain.

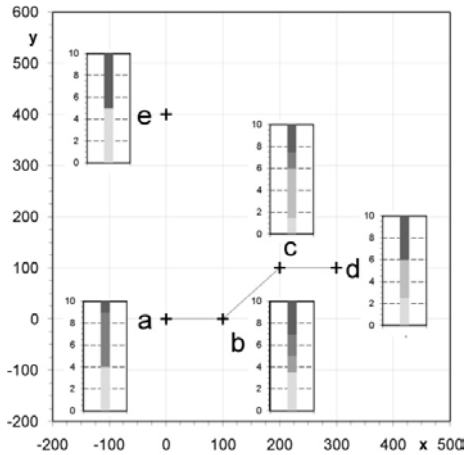

Fig. 5 Position and structuring of imaginary boreholes within the interpolation domain.

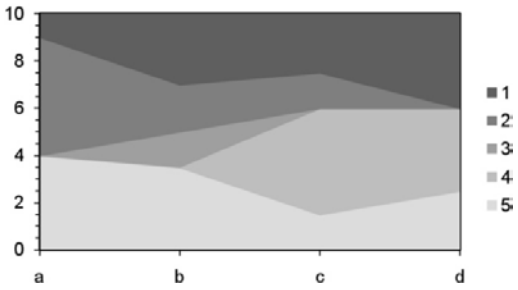

Fig. 6 Possible hydro-geological interpretation following cross section of boreholes a–d in x-direction, not to scale.

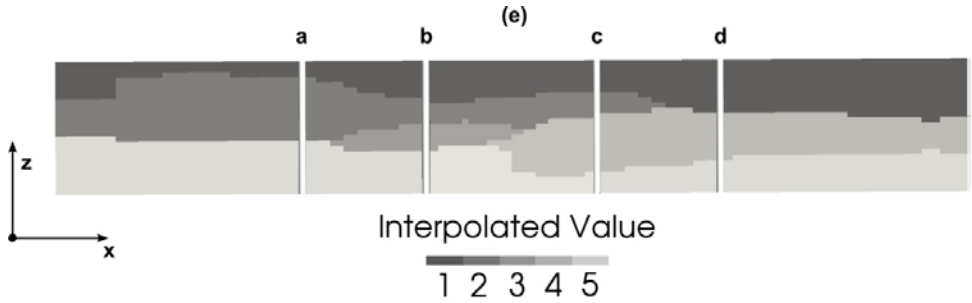

Fig. 7 Interpolation result following cross section of boreholes a–d in x-direction, 10 times vertical exaggeration.

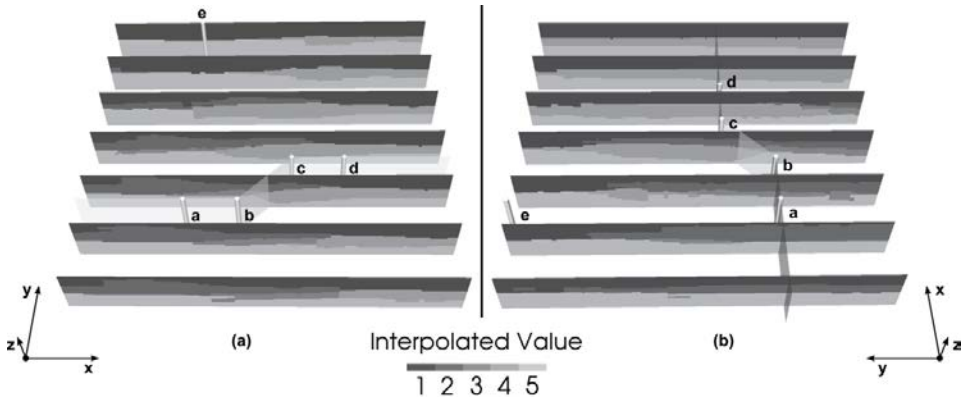

Fig. 8 Three-dimensional presentation of cross sections in x- and y-direction, (a) and (b), respectively, 10 times vertical exaggeration.

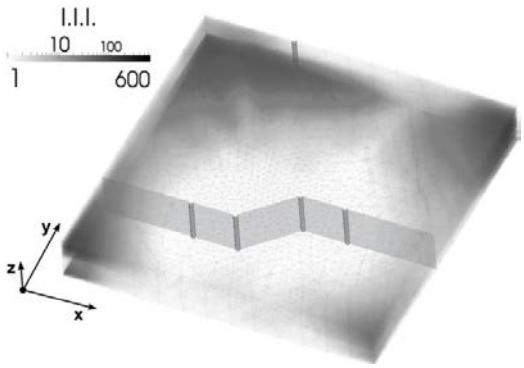

Fig. 9 Three-dimensional presentation of III (logarithmical scale) and grid, 10 times vertical exaggeration.

For the synthetic example, runtime of IA to interpolate 40 100 GP with a mean of 120 LP′ per GP was 51s (approx. 780 interpolated values per second) using approx. 20 MB RAM on an Intel Core2Duo 2.5GHz machine.

Field application

Using information from approx. 50 boreholes and the appendant hydro-geological interpretations of the layered structures in a study area in Oman, IA is applied to a large-scale real-world data set. Analysing the borehole information, 12 distinct hydro-geological materials could be identified covering a wide range of material types from gravelly over silty to clayey sediments. Figure 10 shows the interpolation result: the heterogeneous geological domain mainly consists of two significant layers, i.e. a thin Quaternary, highly permeable layer that thins out toward the coast and below a thick Tertiary, less permeable layer. Additionally, a local hydro-geological characteristic can be determined in the southeast of the study area: the "Ma'awil trough", a relatively large, highly permeable area, which has also been described by several authors using different kinds of data (JICA, 1986; BRGM, 1992; Lakey *et al.*, 1995; Macumber, 1998). Using the interpolation result, a numerical groundwater model for the study area could be calibrated successfully using the open source scientific software package OpenGeoSys (OpenGeoSys, 2011; Walther *et al.*, 2012).

Interpolating the real-world application domain of 126 660 GP with a mean of 66 LP′ per GP took 900s (approx. 140 interpolated values per second) using approx. 50 MB RAM on an Intel Core2Duo 2.5GHz machine.

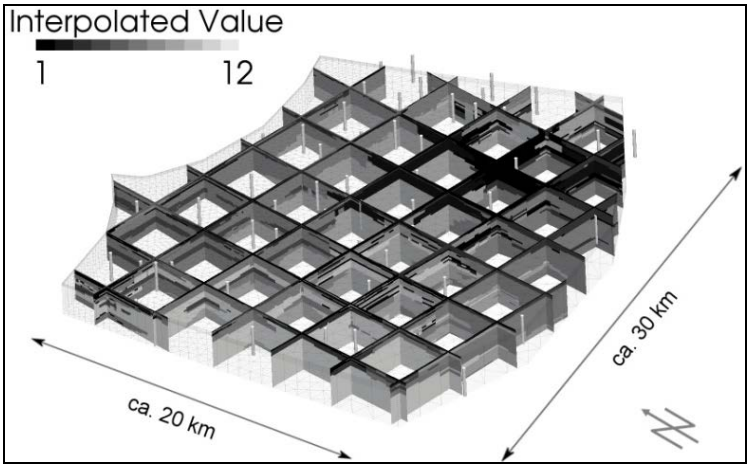

Fig. 10 Three-dimensional visualization of interpolation result, position of borehole information and grid; darker colours mean higher permeability, five times vertical exaggeration.

SUMMARY AND OUTLOOK

We presented a method to interpolate layered, tilted structures in a 3D domain using an extended inverse distance weighting approach. The algorithms implementation and features were shown as well as two applications successfully interpolated using both synthetic and real-world data.

Possible future advancements of the IA include modules to reproduce fractures in bedrock or faulted structures in metamorphic rock. Also, splines could be used to include nonlinear layer pointing. Finally, a profound code review might result in an additional speedup and better performance of the algorithm.

Acknowledgements This work is part of the IWAS joint research project and was funded by the German Federal Ministry of Education and Research (BMBF). The authors acknowledge the

cooperation with the Omani Ministries of Municipalities and Water Resources and appreciate the continuous exchange of data and knowledge.

REFERENCES

Ayvaz, M. T., Karahan, H. & Aral, M. M. (2007) Aquifer parameter and zone structure estimation using kernel-based fuzzy c-means clustering and genetic algorithm. *J. Hydrol.* 343(3–4), 240–253. doi:16/j.jhydrol.2007.06.018.

Bargaoui, K. Z. & Chebbi, A. (2009) Comparison of two kriging interpolation methods applied to spatiotemporal rainfall. *J. Hydrol.* 365(1–2), 56–73. doi:16/j.jhydrol.2008.11.025.

Bartier, P. M. & Keller, C. P. (1996) Multivariate interpolation to incorporate thematic surface data using inverse distance weighting (IDW). *Computers & Geosciences*, 22(7), 795–799. doi:10.1016/0098-3004(96)00021-0.

BRGM (1992) Bureau de Recherches Geologiques et Minieres. Study of a New Organization of Irrigation in Barka-Rumais Area, Data Analysis and Modelling Report. *Technical Report, Ministry of Agriculture and Fisheries.*

Calcagno, P., Chilès, J. P., Courrioux, G. & Guillen, A. (2008) Geological modelling from field data and geological knowledge: Part I. Modelling method coupling 3D potential-field interpolation and geological rules. *Physics of the Earth and Planetary Interiors* 171(1–4), 147–157. doi:16/j.pepi.2008.06.013.

Falivene, O., Cabrera, L. & Sáez, A. (2007) Optimum and robust 3D facies interpolation strategies in a heterogeneous coal zone (Tertiary As Pontes basin, NW Spain). *Int. J. Coal Geology* 71(2–3), 185–208. doi:10.1016/j.coal.2006.08.008.

Dubrule, O. (1984) Comparing splines and kriging. *Computers & Geosciences* 10(2–3), 327–338. doi:16/0098-3004(84)90030-X.

JICA (1986) Hydrologic observation project in the Batinah Coast of Sultanate of Oman, *Final Report*, Volume 4.

Lakey, R., Easton, P & AI Hinai, H. (1995) Eastern Batinah resource assessment. Numerical modeling, stage 1: Data collation and analysis. *MWR.*

Lu, G. Y. & Wong, D. W. (2008) An adaptive inverse-distance weighting spatial interpolation technique. *Computers & Geosciences* 34(9), 1044-1055. doi:10.1016/j.cageo.2007.07.010

Macumber, P.G. (1998) The cable tool program and groundwater flow in the eastern Batinah alluvial aquifer. *Technical Report; Ministry of Water Resources, Oman.*

Ming, J., Pan, M., Qu, H. & Ge, Z. (2010) GSIS: A 3D geological multi-body modeling system from netty cross-sections with topology. *Computers & Geosciences* 36(6), 756–767. doi:10.1016/j.cageo.2009.11.003.

OpenGeoSys (2011) OpenGeoSys Webpage, http://www.opengeosys.net.

Walther, M., Delfs, J. O., Grundmann, J., Kolditz, O., Liedl, R. (2012) Saltwater intrusion modeling: Verification and application to an agricultural coastal arid region in Oman. *J. Computational and Applied Mathematics* 236(18), 4798–4809, ISSN 0377-0427, 10.1016/j.cam.2012.02.008.

Watson, D. F. (1982) Acord: automatic contouring of raw data. *Computers & Geosciences* 8, 97–101.

Yue, T.-X., Du, Z.-P., Song, D.-J. & Gong, Y. (2007) A new method of surface modeling and its application to DEM construction. *Geomorphology* 91(1–2), 161–172. doi:16/j.geomorph.2007.02.006